

A Multi-periodicity and Multi-scale Network for Motor Fault Diagnosis

Pengcheng Xia, Kaiwen Zhang, Yixiang Huang, and Chengliang Liu

*State Key Laboratory of Mechanical System and Vibration,
Shanghai Jiao Tong University, Shanghai, 200240, China*

xpc19960921@sjtu.edu.cn

qq1300221020@sjtu.edu.cn

huang.yixiang@sjtu.edu.cn

chlliu@sjtu.edu.cn

ABSTRACT

Intelligent fault diagnosis of motor is of tremendous significance to ensuring reliable industrial production, and deep learning methods have gained notable achievements recently. Most studies automatically extracted fault information from raw monitoring signals with deep models, whereas the strong periodic temporal information containing in the signals were ignored. To tackle this limitation, a multi-periodicity and multi-scale network is proposed in this paper. 1D monitoring signals are transformed into 2D space with multiple various periods, allowing for the straightforward reflection and modeling of variations both within and between different periods. Multi-scale learning is introduced to extract temporal information from the multi-periodicity representations with multiple scales in a parameter-efficient way. Experiments carried out on a motor fault dataset verified the effectiveness of the proposed method. The results demonstrate that over 99% diagnosis accuracy can be achieved with one-channel vibration signals, and superior performance is obtained under diverse noise conditions compared with other methods.

1. INTRODUCTION

As a key electromechanical device of many important industrial equipment, motor has made a substantial contribution to industrial production. Unforeseen faults are inevitable in practical applications, and they may significantly diminish equipment reliability and potentially lead to catastrophic consequences (Xia, Huang, Tao, Liu, & Liu, 2023). Motor fault diagnosis is a critical approach to facilitate timely maintenance to ensure safe production and extensive methods have been explored to enhance the diagnosis accuracy (Gangsar & Tiwari, 2020).

Xia P. et al. This is an open-access article distributed under the terms of the Creative Commons Attribution 3.0 United States License, which permits unrestricted use, distribution, and reproduction in any medium, provided the original author and source are credited.

With the rapid development of artificial intelligence (AI) techniques, deep learning-based intelligent fault diagnosis have shown great advancements (Lang et al., 2022). These methods learn latent feature representations from raw monitoring signals or time-frequency spectrum without manual feature design and expertise knowledge, and accomplish fault diagnosis task in an automatic and end-to-end way (Xia, Huang, Wang, Zhong, & Liu, 2022). Convolutional neural network (CNN) is the most widely employed type of deep models. It can extract effective features from raw signals or spectrographs with convolutional kernels. For example, Shao et al. (Shao, Yan, Lu, Wang, & Gao, 2020) employed a deep CNN to diagnose faults of induction motors from time-frequency images generated through continuous wavelet transform of the vibration and current signals. Wang et al. (Wang, Liu, Hu, & Chen, 2021) proposed a cascade CNN (C-CNN) for motor fault diagnosis, which possessed a cascade structure and dilated convolution operations to extract features from multiple scales. Tao et al. (Tao et al., 2021) utilized deep CNNs with residual connections for motor fault diagnosis with signals from multiple sensors, and a decision fusion strategy was proposed to obtain more reliable final diagnosis results. These deep learning-based methods demonstrated promising performance in different fault diagnosis tasks of motors.

In addition to the CNN, several other types of deep models have been successfully applied to motor fault diagnosis. The most popular recurrent neural network, that is, long short-term memory (LSTM) network was utilized to capture long-range temporal information from raw signals and diagnose motor faults (Xiao et al., 2018). Some studies introduced graph neural networks (GNNs) to learn fault information from graphs constructed by monitoring signals (Tang et al., 2021).

However, the LSTM is limited in its capability to model tem-

poral dependencies from signals with excessively long sequences, and the GNN is usually utilized based on manually-designed graphs, which involve extensive expertise knowledge. Although CNN is suitable for fault information modeling from monitoring signals, a crucial characteristic in sensory signals of motors is overlooked. Specifically, as motor is a rotational machine, the monitoring signals such as vibration and current signals inherently exhibit strong periodicity. Fault patterns will be not only manifested within each single period but also between different periods. More specifically, some types of faults may lead to variations across various periods, whereas these inter-period variations are challenging for CNNs to capture, resulting in failure of extracting specific important fault features.

To tackle these limitations, a multi-periodicity and multi-scale network (MPMSN) is proposed for motor fault diagnosis. It aims to learn temporal variations both within and between multiple periods in the monitoring signal sequences for motor fault diagnosis performance enhancement based on the TimesNet proposed for time series analysis (Wu et al., 2023). The 1D signal sequences are firstly transformed into multiple 2D tensors with different periods determined by the dominant frequencies through fast Fourier Transform (FFT). Subsequently, the variations within and across periods can be explicitly reflected, facilitating the multi-periodicity modeling. Moreover, multi-scale learning is employed to extract feature from multiple scales in the 2D space for adaptive and robust feature learning. The multi-periodicity latent information is modeled with a parameter-efficient multi-scale network, and is aggregated adaptively to produce diagnosis results. The proposed MPMSN method is validated on an experimental dataset of induction motor faults, and results show the effectiveness of the method and superiority under diverse noise conditions.

2. METHODOLOGY

The proposed MPMSN primarily consists of stacked TimesBlocks, which transforms 1D signals into the 2D space and utilizes a multi-scale Inception block (Szegedy et al., 2015) to extract features, and aggregate multi-periodicity features for subsequent processing. In this section, the principle of TimesBlock is firstly introduced, and subsequently the structure of the MPMSN is described.

2.1. Multi-periodicity Modeling with TimesBlock

Figure 1 illustrates the principle of the multi-periodicity modeling process. The input signal sequence is firstly transformed into multiple 2D tensors for multi-periodicity processing, and then transformed back into 1D series for information aggregation. In the 2D space, the variations within and between multiple periods can be simultaneously captured with 2D convolutional kernels.

For the input signal sequence $\mathbf{x} \in \mathbb{R}^{L \times C}$ with C channels and the length of L , the periods for transformation are firstly determined through FFT. The single sided frequency spectrum is obtained as follows.

$$\mathbf{A} = \frac{1}{C} \sum_{c=1}^C |\text{FFT}(\mathbf{x}_c)|, \quad (1)$$

where \mathbf{x}_c denotes the c -th channel of the input sequence, and $|\text{FFT}(\cdot)|$ denotes the amplitude values of the single sided FFT spectrum, i.e., $\mathbf{A} \in \mathbb{R}^{\lfloor \frac{L}{2} \rfloor + 1}$. Then, k frequencies with the top- k spectrum amplitude values are selected, formulated as follows.

$$\{f_1, f_2, \dots, f_k\} = \text{argTopk}(\mathbf{A}). \quad (2)$$

As a result, k corresponding periods can be determined by these k frequencies as follows.

$$p_i = \lceil \frac{L}{f_i} \rceil, i \in 1, 2, \dots, k. \quad (3)$$

Afterwards, the input sequence is reshaped into k 2D tensors, where the row number of the i -th tensor is the i -th period, i.e., p_i . To make the sequence compatible for the reshape operation, zero-padding is performed to extend the sequence by zero values along the time dimension to the length of $p_i \cdot f_i$. Consequently, k 2D tensors $\mathbf{z}_1, \mathbf{z}_2, \dots, \mathbf{z}_k$ are obtained, where $\mathbf{z}_i \in \mathbb{R}^{p_i \times f_i}$.

These k 2D tensors with multiple periods will be processed by a shared Inception block for efficient parameters. The Inception block utilizes multi-scale 2D convolutional kernels to capture variations within and between periods from multiple scales. Subsequently, the extracted 2D feature representations are reshaped back into 1D tensors $\hat{\mathbf{x}}_i \in \mathbb{R}^{L \times d}$, which are truncated into the original sequence length L , and d denotes the kernel number in the Inception block.

The multi-periodicity 1D feature representations are subsequently fused to form comprehensive features. These 1D tensors are aggregated adaptively with weighted proportion, where the weights are depended on the frequency amplitudes in the spectrum of the corresponding periods. Concretely, the aggregation weights are calculated as follow.

$$w_i = \frac{e^{A_{f_i}}}{\sum_{j=1}^k e^{A_{f_j}}}, \quad (4)$$

where A_{f_i} denotes the amplitude of frequency f_i in the spectrum \mathbf{A} . Consequently, the final aggregated representation is obtained as

$$\hat{\mathbf{x}} = \sum_{j=1}^k w_j \cdot \hat{\mathbf{x}}_j. \quad (5)$$

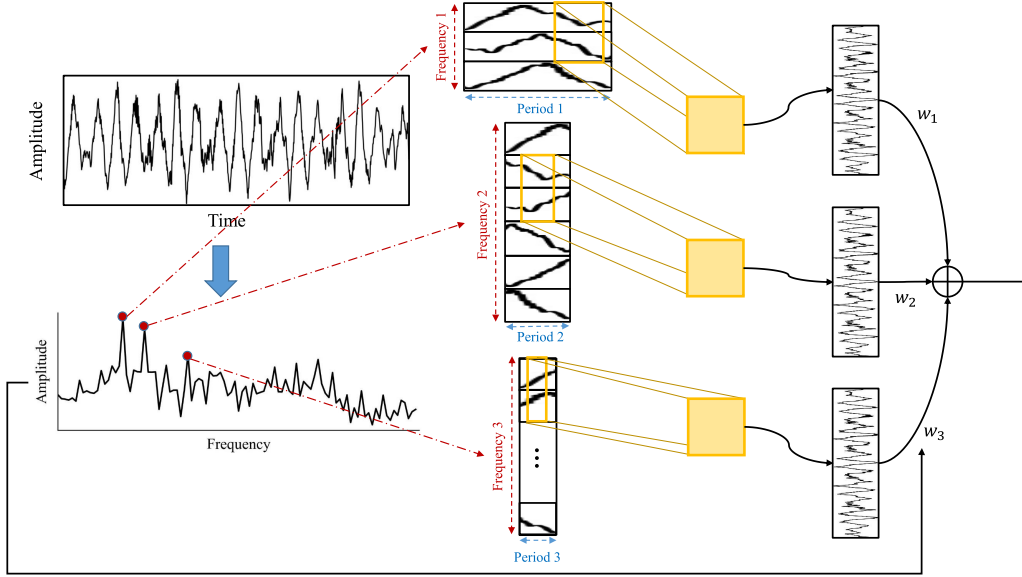


Figure 1. Principle illustration of the multi-periodicity modeling process with TimesBlock.

2.2. MPMSN

The MPMSN consists of several stacked TimesBlocks with residual connection. The structure of a single residual block is illustrated as Figure 2. Two stacked Inception blocks are utilized to extract multi-scale features from the multi-periodicity 2D representations. Notably, the Inception blocks are shared for 2D tensors with different periods in a parameter-efficient way. In the Inception block, f parallel convolutional branches are employed to extract multi-scale features with convolutional sizes of 1×1 , 3×3 , \dots , and $(2f + 1) \times (2f + 1)$, respectively. Subsequently, these f feature representations are fused by calculating the average representations among all the branches. Between the two Inception blocks, a Gaussian Error Linear Unit (GELU) (Hendrycks & Gimpel, 2016) is introduced as the activation function.

In the MPMSN, the residual connection is utilized between the original 1D sequences and the aggregated 1D representations, formulated as

$$\mathbf{x}^l = \mathbf{x}^{l-1} + \hat{\mathbf{x}}^{l-1}, \quad (6)$$

where the superscript l denoted the l -th residual block, and \mathbf{x} and $\hat{\mathbf{x}}$ are the original 1D sequences and the aggregated 1D representations, respectively. Finally, the output of the last residual block is processed by a fully connected softmax classifier to obtain the final diagnosis results. And the entire network is trained by minimizing the cross-entropy loss.

3. EXPERIMENTAL VERIFICATION

To validate the proposed MPMSN method, a motor fault dataset is utilized for verification. In this section, the experi-

ment details are described and the results are presented.

3.1. Dataset Description

The motor fault dataset was constructed through experiments on a Drivetrain Dynamics Simulator (DDS) platform shown as Figure 3. Eight test motors with various fault states were utilized to acquire monitoring signals under different health states, which were normal state (N), rotor parallel misalignment fault (PMR), stator winding fault (SWF), rotor unbalance fault (RU), rotor angular misalignment fault (AMR), bearing fault (BF), rotor bowed fault (RB), and broken rotor bar fault (BRB). The rotating speed of the motor, which was 1800 RPM (30 Hz) in this experiment, was controlled by the speed controller. And a load of 3.4 N·m was applied by the electromagnetic brake. The axial vibration signals of the motor were collected by an accelerometer placed on the end cover and the data acquisition device with the sampling rate of 5120 Hz. After data acquisition and segmentation, there were 200 samples for each health state, and each of these samples had a length of 1024 points. These samples were randomly partitioned into a training set, validation set, and testing set with a proportion of 7:1:2.

3.2. Experiment Details

As only one channel of vibration signals are used for fault diagnosis, the input sequences possess a dimension of 1024×1 . Top-3 frequencies are selected for multi-periodicity transformation, i.e., $k = 3$ in the experiments. Take a sample of normal state as example, which is shown as Figure 4(a), and the frequency spectrum is illustrated as Figure 4(b). It can be observed that the top-3 frequencies are 90 Hz, 120 Hz, and

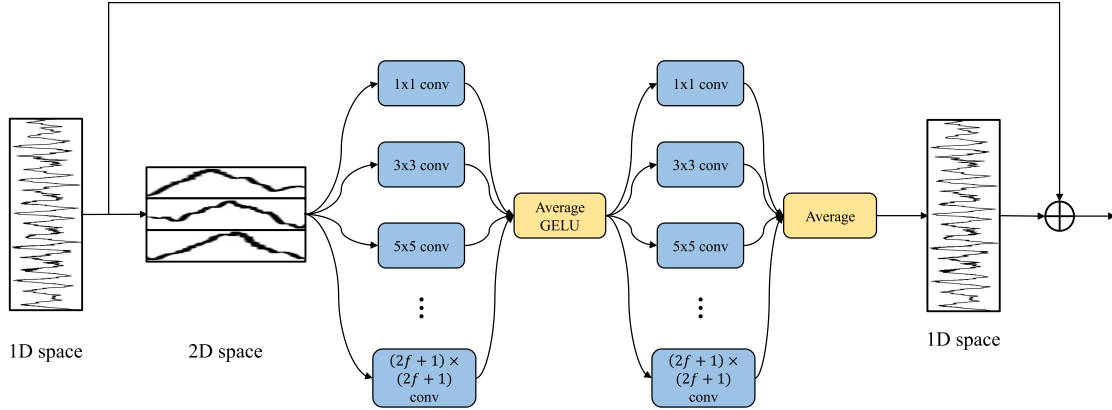


Figure 2. Structure illustration of the MPMSN. Only one Timesblock is presented.

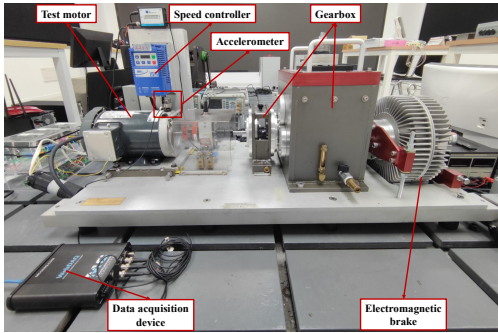


Figure 3. Motor fault experimental platform.

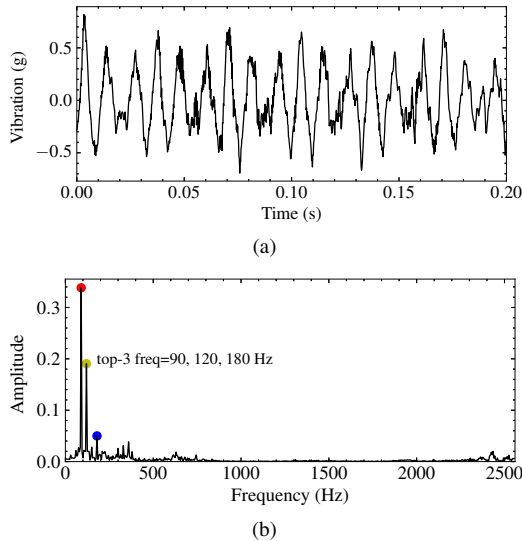
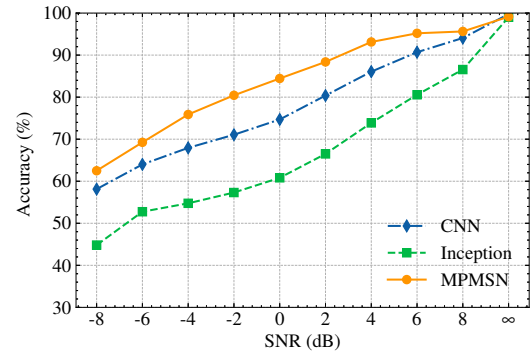


Figure 4. Signal sequence of a sample of the normal state (a) and its single sided frequency spectrum (b).

180 Hz, respectively, which are 3 times, 4 times, and 6 times the rotating frequency. Therefore, the input signal sequence will be transformed into three 2D tensors with lengths of 29,

Figure 5. Fault diagnosis results of three methods under different noise conditions. ∞ represents no additional noise is added.

43, and 57 points accordingly in the first TimesBlock.

In this paper, the MPMSN containing two TimesBlocks are constructed. In each Inception block, there are 5 branches with different kernel sizes, i.e., $f = 5$, and the kernel sizes of the two Inception blocks in each TimesBlock are set to 64 and 32, respectively. After the second TimesBlock, the dimensionality is reduced to 4 through global average pooling (GAP), and the representations are subsequently processed by a fully connected layer to obtain the final classification results. The mini-batch size is set to 128. Adam optimizer is utilized with an initial learning rate of 0.001, which is reduced to 0.0001 after training for 10 epochs, and the training process ended after 20 epochs. All the experiments are conducted for five times to avoid the influence of randomness.

3.3. Experiment Results

After trained on the training set, the MPMSN model achieves 99.13% diagnosis accuracy of the 8 fault states on the testing set, demonstrating the strong capacity of motor fault diagnosis. To verify the model performance under industrial

Table 1. Recall (R), Precision (P), and F1 value of three methods under different noise conditions. ∞ represents no additional noise is added.

Method	Metric	-8 dB	-6 dB	-4 dB	-2 dB	0 dB	2 dB	4 dB	6 dB	8 dB	∞
CNN	R	58.13	64.00	67.94	71.06	74.69	80.38	86.06	90.69	94.06	99.75
	P	58.34	63.80	67.71	70.79	74.59	80.66	86.94	91.55	94.86	99.76
	F1	57.86	63.50	67.24	70.33	73.86	79.73	85.63	90.46	93.97	99.75
Inception	R	44.81	52.75	54.75	57.31	60.81	66.50	73.88	80.56	86.56	99.00
	P	42.82	52.25	54.89	58.40	62.33	68.24	76.19	83.77	89.30	99.06
	F1	41.49	50.30	52.04	54.67	58.36	64.47	72.44	79.63	85.72	99.00
MPMSN	R	62.50	69.25	75.88	80.44	84.44	88.38	93.13	95.19	95.63	99.13
	P	63.44	69.68	76.51	81.84	85.36	89.37	94.12	95.85	96.20	99.17
	F1	62.40	68.16	74.77	79.36	83.84	88.04	92.99	95.13	95.59	99.12

high-noise scenarios, Gaussian white noise of various signal-to-noise rates (SNR) from -8 to 8 is injected to the original vibration signals for further experiments. To show the model effectiveness, other two deep learning models are implemented for comparative study. The first one is a deep CNN, which has four convolutional layers combined with batch normalization (BN), and the softmax classifier is the same as that of the MPMSN. Another is a 1D Inception network, the primary difference between which and the MPMSN is that the multi-periodicity transformations from 1D sequences into the 2D space are removed and the 1D convolutional operations are performed along the time direction straightforward. The results of the 1D Inception can verify the effectiveness of the multi-periodicity modeling in the 2D space.

Figure 5 demonstrates the diagnosis results of these three methods under various noise conditions. It can be observed that the diagnosis accuracy of the three methods decreases as additional noise increases. The MPMSN can still achieves over 60% diagnosis accuracy under the condition with extremely high noise when the SNR is -8 dB, and the accuracy under almost all noise conditions outperforms the CNN and Inception network. The diagnosis results in terms of other three metrics, including Recall (R), Precision (P), and F1 value, are demonstrated in Table 1. It shows that the three methods achieve close results in terms of three metrics, and the results of MPMSN are superior to that of CNN and Inception, demonstrating the superiority of the MPMSN under noisy conditions which are common in industry.

Figure 6 presents the confusion matrices of three methods under two noise conditions. It is observed that three methods can almost recognize all samples accurately. However, when the noise of 0 dB SNR is added, noticeable misclassifications occur for most fault categories. Three methods can only accurately recognize the BF and RB states. For other categories, the MPMSN achieves higher recognition accuracy compared with the other two methods.

The number of periods used in the multi-periodicity transformation, i.e., k , is a critical parameter in the MPMSN method.

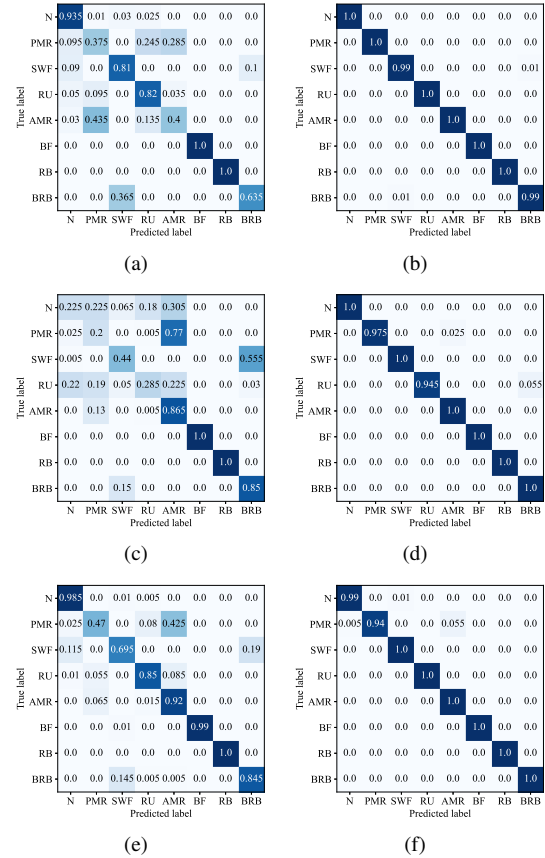


Figure 6. Confusion matrices. (a)-(b) CNN, (c)-(d) Inception network, (e)-(f) MPMSN. (a), (c), and (e) are under the noise condition with the SNR of 0 dB. (b), (d), and (f) are with no additional noise.

Experiments are conducted to investigate the effects of different k , where k is chosen from 1 to 5. Figure 7 presents the diagnosis accuracy with different k with no additional noise. It can be seen that the accuracy with only one period is significant lower than with multiple periods. When k is larger than 1, the accuracy can reach higher than 98%. The best result is achieved when $k = 3$, and larger k results in accuracy

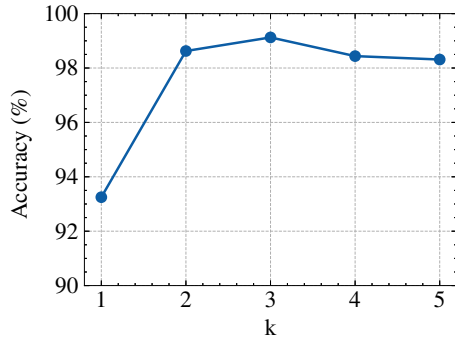


Figure 7. Diagnosis accuracy with different period number k .

decline.

4. CONCLUSION

In this paper, a multi-periodicity and multi-scale network (MPMSN) is proposed for motor fault diagnosis. It transforms 1D monitoring signals into the 2D space with multiple various periods determined through FFT, and the variations both within and between various periods can be captured by convolutional networks. Multi-scale learning is also introduced to extract feature representations from the 2D tensors from multiple scales. A motor fault experimental dataset is utilized for method validation, and results show that over 99% diagnosis accuracy can be achieved for eight fault states. Compared with CNN and 1D Inception network, the MPMSN also obtained superior performance in terms of recognition accuracy and other three common metrics under different noise conditions. The results show the effectiveness and promising capacity of MPMSN to deal with motor fault diagnosis problems in industrial applications.

ACKNOWLEDGMENT

This work was supported by the National Natural Science Foundation of China (No. 51975356) and the Shanghai Municipal Science and Technology Major Project, PR China (No. 2021SHZDZX0102).

REFERENCES

- Gangsar, P., & Tiwari, R. (2020). Signal based condition monitoring techniques for fault detection and diagnosis of induction motors: A state-of-the-art review [Journal Article]. *Mechanical Systems and Signal Processing*, 144. doi: ARTN 106908 10.1016/j.ymssp.2020.106908
- Hendrycks, D., & Gimpel, K. (2016). Gaussian error linear units (gelus). *arXiv preprint arXiv:1606.08415*.
- Lang, W., Hu, Y., Gong, C., Zhang, X., Xu, H., & Deng, J. (2022). Artificial intelligence-based technique for fault detection and diagnosis of ev motors: A review [Journal Article]. *IEEE Transactions on Transportation Electrification*, 8(1), 384-406. doi: 10.1109/tte.2021.3110318
- Shao, S., Yan, R., Lu, Y., Wang, P., & Gao, R. X. (2020). Dcnn-based multi-signal induction motor fault diagnosis [Journal Article]. *IEEE Transactions on Instrumentation and Measurement*, 69(6), 2658-2669. doi: 10.1109/tim.2019.2925247
- Szegedy, C., Liu, W., Jia, Y., Sermanet, P., Reed, S., Anguelov, D., ... Rabinovich, A. (2015). Going deeper with convolutions. In *2015 IEEE conference on computer vision and pattern recognition (CVPR)* (p. 1-9). doi: 10.1109/CVPR.2015.7298594
- Tang, Y., Zhang, X., Qin, G., Long, Z., Huang, S., Song, D., & Shao, H. (2021). Graph cardinality preserved attention network for fault diagnosis of induction motor under varying speed and load condition [Journal Article]. *IEEE Transactions on Industrial Informatics*, 1-1. doi: 10.1109/tii.2021.3112696
- Tao, Z., Xia, P., Huang, Y., Xiao, D., Wuang, Y., Zhong, Z., & Liu, C. (2021). Induction motor fault diagnosis based on multi-sensor fusion under high noise and sensor failure condition [Conference Proceedings]. In *2021 global reliability and prognostics and health management (phm-nanjing)* (p. 1-8). doi: 10.1109/PHM-Nanjing52125.2021.9612787
- Wang, F., Liu, R. N., Hu, Q. H., & Chen, X. F. (2021). Cascade convolutional neural network with progressive optimization for motor fault diagnosis under nonstationary conditions [Journal Article]. *IEEE Transactions on Industrial Informatics*, 17(4), 2511-2521. doi: 10.1109/Tii.2020.3003353
- Wu, H., Hu, T., Liu, Y., Zhou, H., Wang, J., & Long, M. (2023). Timesnet: Temporal 2d-variation modeling for general time series analysis. In *The eleventh international conference on learning representations*.
- Xia, P., Huang, Y., Tao, Z., Liu, C., & Liu, J. (2023). A digital twin-enhanced semi-supervised framework for motor fault diagnosis based on phase-contrastive current dot pattern [Journal Article]. *Reliability Engineering & System Safety*, 235, 109256. doi: 10.1016/j.res.2023.109256
- Xia, P., Huang, Y., Wang, Y., Zhong, Z., & Liu, C. (2022). Selective kernel prototypical network for few-shot motor fault diagnosis with unseen faults [Conference Proceedings]. In *2022 global reliability and prognostics and health management (phm-yantai)* (p. 1-7). doi: 10.1109/PHM-Yantai55411.2022.9942130
- Xiao, D., Huang, Y., Zhang, X., Shi, H., Liu, C., & Li, Y. (2018). Fault diagnosis of asynchronous motors based on lstm neural network. In *2018 prognostics and system health management conference (phm-chongqing)* (p. 540-545). doi: 10.1109/PHM-Chongqing.2018.00098